

## Article

# Recycling Aged Asphalt Using Hard Asphalt Binder for Hot-Mixing Recycled Asphalt Mixture

Jian Zhou, Jing Li, Guoqiang Liu, Tao Yang and Yongli Zhao \*

School of Transportation, Southeast University, Nanjing 210096, China; 230139228@seu.edu.cn (J.Z.); 230149195@seu.edu.cn (J.L.); guoqiangliu2016@seu.edu.cn (G.L.); ytaochd@126.com (T.Y.)

\* Correspondence: yonglizhao2016@126.com

**Abstract:** Increasing the content of reclaimed asphalt pavement material (RAP) in hot-mix recycled asphalt mixture (RHMA) with a satisfactory performance has been a hot topic in recent years. In this study, the performances of Trinidad lake asphalt (TLA), virgin asphalt binder, and aged asphalt binder were first compared, and then the modification mechanism of TLA on virgin asphalt and aged asphalt was explored. Furthermore, the RHMA was designed in accordance with the French norm NF P 98-140 containing 50% and 100% RAP, and their high-temperature stability, low-temperature cracking resistance, and fatigue performances were tested to be compared with the conventional dense gradation AC-20 asphalt mixture. The results show that the addition of TLA changes the component proportion of virgin asphalt binder, but no new functional groups are produced. The hard asphalt binder modified by TLA has a better rutting resistance, while the fatigue and cracking resistance is lower, compared to both aged and virgin asphalt. The high-modulus design concept of RHMA is a promising way to increase the RAP content in RHMA with acceptable performance. Generally, the RHMA with 50% RAP has similar properties to AC-20. And, when the RAP content reaches 100%, the high- and low-temperature performance and anti-fatigue performance of RHMA are better than AC-20 mixture. Thus, recycling aged asphalt using hard asphalt binder for hot-mixing recycled asphalt mixture to increase the RAP content is feasible.

**Keywords:** Trinidad lake asphalt; aged asphalt; hot-mix recycled asphalt mixture; reclaimed asphalt pavement; high-modulus asphalt mixture

check for  
updates

**Citation:** Zhou, J.; Li, J.; Liu, G.; Yang, T.; Zhao, Y. Recycling Aged Asphalt Using Hard Asphalt Binder for Hot-Mixing Recycled Asphalt Mixture. *Appl. Sci.* **2021**, *11*, 5698. <https://doi.org/10.3390/app11125698>

Academic Editor: Amir Tabakovic

Received: 24 April 2021

Accepted: 17 June 2021

Published: 19 June 2021

**Publisher's Note:** MDPI stays neutral with regard to jurisdictional claims in published maps and institutional affiliations.



**Copyright:** © 2021 by the authors. Licensee MDPI, Basel, Switzerland. This article is an open access article distributed under the terms and conditions of the Creative Commons Attribution (CC BY) license (<https://creativecommons.org/licenses/by/4.0/>).

## 1. Introduction

Recycling the old asphalt pavement is a common operation used worldwide for saving natural materials, investment, and energy in highway maintenance projects [1–4]. In practice, the hot-mix recycled asphalt mixture (RHMA) has similar durability and performance to the conventional dense asphalt mixture if the RAP content is limited at 10–40%, depending on the design of mixture [5–7]. According to recent official data, China produces approximately 790 million tons of reclaimed asphalt pavement (RAP) per year through asphalt pavement rehabilitation projects [8]. This figure is expected to significantly increase in the next five years as the demand for road maintenance is increasing. Following the issuance of the most stringent environmental protection law in China's history, the exploitation of natural stone has been significantly restricted, leading to an estimated capacity reduction of over 60%. Consequently, in some parts of the country, such as the Jiangxi Province, the price of natural aggregate has nearly tripled in the past five years [9]. Thus, the Chinese transportation infrastructure sector faces years of ineffective reuse of accumulated RAP and increasing natural aggregate costs in future asphalt pavement rehabilitation projects. Therefore, increasing the RAP content in RHMA has attracted increasing attention over the past few years [10,11].

Although the aged asphalt binder in RAP is a considerable asset for construction, the incorporation of RAP could potentially reduce the durability in terms of fatigue resistance, low-temperature cracking resistance, and moisture stability due to its poor rheological

properties after volatilization and oxidation in the field [12]. To this end, the most widely and traditional solution is adding rejuvenators or using soft asphalt binder as the modifier to recover the performance of aged asphalt binder [13,14]. This solution was shown to be effective in previous publications and engineering projects. However, when RAP content reaches a high percentage (for example, over 50% by the weight of RHMA), the extra softening additives could reduce the rutting resistance of RHMA [15,16]. Thus, the use of a high percentage of RAP in RHMA has not been properly addressed in current recycling technology.

To overcome the negative effect of softening additives on RHMA, previous studies reported that the high-modulus asphalt concrete (HMAC) that originated in France in the early 1980s could be a potential solution [17]. The basic design concept of high-modulus asphalt mixtures is that through the use of hard-grade asphalt binder (with a penetration of about 10–20), fine aggregate gradation, high asphalt binder content (about 6%), and low porosity (generally 3%), the high-modulus asphalt mixture is obtained through the high modulus properties of the hard-grade asphalt binder itself [18]. For example, Ma et al. indicated that the HMAC has a higher binder/aggregate ratio, lower void content, and finer aggregate gradation compared to the conventional dense asphalt concrete [19]. The results show that the addition of RAP can be incorporated into HMAC at relatively higher contents, due to the similar stiffness between the aged asphalt binder in RAP and the high-modulus asphalt binder. To achieve good rutting resistance, hard asphalt binder is a suitable modifier of HMAC. In most cases, the hard asphalt is produced in refineries, and it also can be obtained by blending the virgin asphalt and natural asphaltite, for example, Trinidad lake or Gilsonite-like materials, whose penetration is in range of 8–28 (0.1 mm) [20]. Thus, the design concept of HMAC has the potential of incorporating more RAP contents in the asphalt mixture. However, using hard asphalt binder as the rejuvenator to recover the aged binder is rarely reported in previous studies. The traditional asphalt mixture regeneration technology is to add rejuvenator or soft asphalt to reduce the viscosity of the aged asphalt, thereby restoring its performance. Therefore, this topic may go against the concept of the traditional solutions. The objectives of this work can be summarized as follows.

- Compare the performances of Trinidad lake asphalt, virgin asphalt binder, hard asphalt binder, aged asphalt binder, and recovered asphalt binder.
- Reveal the modification mechanism of Trinidad lake asphalt on aged asphalt binder.
- Verify the feasibility of increasing RAP content in RHMA by using the concept of HMAC.

## 2. Experiments

### 2.1. Materials

#### 2.1.1. Binder

The TH-70# virgin asphalt binder produced by Xinjiang Tarim Petrochemical Co., Ltd, Urumqi, China, was used. Its performance was tested according to a Chinese specification entitled Standard Test Methods of Bitumen and Bituminous Mixtures for Highway Engineering (JTG E20-2011), and the results are shown in Table 1.

Aged binder was obtained using the thin film oven test (TFOT), and each virgin asphalt binder sample with 3.2 mm thickness of asphalt film (50 g) was placed in the oven at  $163.5 \pm 0.5$  °C for a designated duration. To create samples with different aging levels, the heating durations of virgin asphalt binder were 0 h, 5 h, 12 h, 19 h, and 26 h, while the penetration of samples after heating was 64.2, 48.6, 42.4, 34.2, 27.5, respectively.

The hard asphalt binder was used as newly-added virgin asphalt binder in the recycled mixture for recovering the performances of aged asphalt binder. The hard asphalt binder was blended with virgin asphalt binder and Trinidad lake asphalt (TLA). TLA is a stiffer binder with high modulus and poor workability. It is a common modifier for producing hard asphalt binder. The basic performance of TLA was tested according to JTG E20-2011, and the results are shown in Table 2. The TLA was cut into the 1 cm diameter pieces. Virgin

asphalt binder and TLA were respectively heated to 150 °C, and then they were mixed using a high-speed shear mixer for 15 min at 165 °C to reach a uniform state.

**Table 1.** Typical characteristics of TH-70# asphalt binder.

Item	TH-70#	Test Methods
Penetration at 25 °C (0.1 mm)	64.2	ASTM D5
Softening point (°C)	49.0	ASTM D36
Ductility at 15 °C (cm)	>100	ASTM D113
After thin film oven test (TFOT for short, 163 °C, 5 h)		
Mass loss (%)	0.21	ASTM D2872
Penetration at 25 °C (0.1 mm)	48.6	ASTM D5
Softening point (°C)	60.5	ASTM D36
Ductility at 15 °C (cm)	40.1	ASTM D113

**Table 2.** Typical characteristics of Trinidad lake asphalt (TLA).

Item	TLA	Specification
Penetration at 25 °C (0.1 mm)	2.5	0–5
Softening point (°C)	95.0	≥90
Ductility at 15 °C (cm)	-	-
Ash content (%)	19.2	-
Density (g/m <sup>3</sup> )	1.383	1.3–1.5
After TFOT (163 °C, 5 h)		
Mass loss (%)	0.24	<2.0
Penetration ratio (%)	81	≥50

To achieve the objectives of this study, 11 kinds of asphalt binder samples were prepared or used for the laboratory tests. To better organize and introduce this study's work, the specific component, mark, and description of the asphalt binder samples are listed in Table 3.

**Table 3.** Details of the prepared asphalt binder samples.

Number	Description	Mark	Component
1	Virgin asphalt (VA) binder, TH-70#	VA	100% VA
2	Trinidad lake asphalt (TLA), the modifier for virgin asphalt binder to produce the hard asphalt (HA) binder	TLA	100% TLA
3	Hard asphalt binder, produced by TLA and VA, used as newly-added virgin asphalt binder for recycled mixture	HA	40% TLA + 60% VA
4	Aged asphalt binder, obtained by heating VA, numbered by their aging hours	A5h A12h A19h A26h	100% aged asphalt binder
5	Recycled asphalt binder, produced by mixing the different aging level of asphalt binder with HA	A5h + HA A12h + HA A19h + HA A26h + HA	50% aged asphalt binder +50% HA

### 2.1.2. Mixture

Research shows that the asphalt mixture with a finer gradation and a higher asphalt binder content has better low-temperature crack resistance and fatigue performance [21]. Therefore, for different RAP contents, different asphalt mixture gradations were designed in this paper. The greater the RAP content, the finer the asphalt mixture gradation. Three mixtures were designed and tested in this work: (i) the conventional hot-mix dense asphalt mixture using natural aggregates, AC-20; hot-mix recycled asphalt mixture designed with EME-20 (a high-modulus asphalt mixture originally recommended by the French industry) containing (ii) 50% reclaimed asphalt pavement (RAP), and (iii) 100% RAP. The designed aggregate gradation is shown in Figure 1.

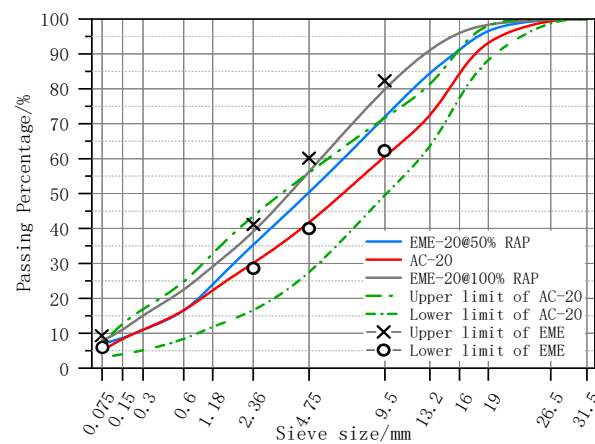


Figure 1. The aggregate gradation of the three designed mixtures.

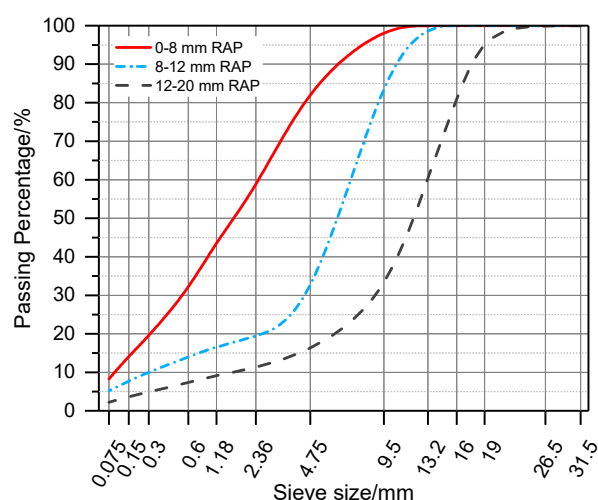
The RAP was collected from a pavement maintenance project; it was then sieved into three classifications: 0–8, 8–12, and 12–20 mm. The aged binder contained in the RAP was extracted from the aggregates according to ASTM D2172-05, and its properties are listed in Table 4. The gradation of three classifications was determined according to ASTM C136, and the results are shown in Figure 2. The gradation was then used in the recycled mixture design by adjusting the ratio of the three classifications. In addition, the asphalt content of the three RAP classifications was tested, and the results were 6.42% (0–8 mm), 3.21% (8–12 mm), and 2.05% (12–20 mm). The physical properties of the virgin and old aggregates are shown in Table 5. The produced hard asphalt (HA), made with 40% TLA and 60% virgin asphalt (VA) was used as the newly-added binder for EME-20@50%RAP and EME-20@100%RAP. The performance of HA is listed in Table 6. Based on the Marshall test, the optimal asphalt contents for AC-20, EME-20@50%RAP, and EME-20@100%RAP were determined. Details are shown in Table 7.

Table 4. The performances of aged asphalt binder extracted from reclaimed asphalt pavement (RAP).

Penetration at 25 °C (0.1 mm)	Softening Point (°C)	Ductility at 15 °C (cm)	Density (g/m <sup>3</sup> )
27	57	21	1.44

Table 5. Physical properties of the aggregates tested according to JTG E42—2005.

Properties	Limestone		RAP Aggregates		Mineral Filler	Test Method
	Coarse	Fine	Coarse	Fine		
Bulk-specific gravity (kg/m <sup>3</sup> )	2751	2715	2720	2622	2648	T0308
Flat-elongated Particles (%)	11.4	-	13.5	-	-	T0311
Water absorption (%)	0.5	-	0.4	-	-	T0308
Crush value (%)	12.6	-	14.2	-	-	T0316
LA abrasion (%)	22	-	24	-	-	T0317



**Figure 2.** Gradation of the aggregates in the three RAP classifications.

**Table 6.** Typical characteristics of used hard asphalt binder.

Item	HA	Specification
Penetration at 25 °C (0.1 mm)	31	20–40
Softening point (°C)	59	≥54
Ductility at 15 °C (cm)	45	-
Density (g/m <sup>3</sup> )	1.42	1.3–1.5
After TFOT (163 °C, 5 h)	Mass loss (%)	0.22
		<2.0

**Table 7.** Asphalt contents of the three mixtures.

Mixtures	Newly-Added Binder	Optimal Binder/Aggregate Ratio	Newly-Added Binder/Aggregate Ratio (in Mass of Recycled Mixture)
AC-20	VA	4.20%	0
EME-20@50%RAP	HA	5.50%	2.79%
EME-20@100%RAP	HA	6.10%	1.36%

## 2.2. Test Methods

### 2.2.1. Dynamic Modulus Test

The objective of the dynamic modulus test is to determine the optimal TLA content in hard asphalt binder considering the improvement of hard asphalt binder on the dynamic modulus of recycled asphalt mixture (RHMA). The LPC Bituminous Mixture Design Guide requires that the dynamic modulus of the high-modulus asphalt mixture is over 14,000 MPa under the conditions of a temperature of 15 °C and a load frequency of 10 Hz [7]. On the other hand, considering that TLA is more expensive than ordinary asphalt, the minimum TLA content that meets the above requirements is the optimal TLA content in hard asphalt. Therefore, the optimal TLA can be determined when the modulus of RHMA reaches 14,000 MPa under 15 °C, 10Hz. A UTM-35 test machine was used, and the investigated frequency was 0–25 Hz. The specimens were prepared with EME-20@50%RAP as it was previously introduced in Table 7, wherein the TLA content in hard asphalt binder was 30%, 40%, 50%, and 70%. The RHMA specimens were compacted using a gyrator compactor. The diameter was 150 mm, and the height was 170 mm. The specimens were cored to a diameter of 100 mm and a height of 150 mm, as shown in Figure 3.

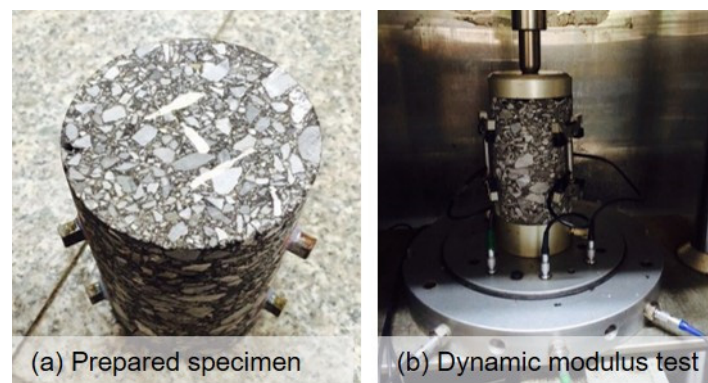


**Figure 3.** The testing of the dynamic modulus of the recycled asphalt mixture.

### 2.2.2. Rheology Test

A dynamic shear rheometer (DSR) was used to evaluate the high-temperature performance of asphalt binder samples according to AASHTO T315. The temperature sweep mode was used to investigate the performance of samples under 58–82 °C. The complex modulus  $G^*$  and phase angle  $\delta$  were recorded to calculate the fatigue factor ( $G^* \sin \delta$ ) and rutting-resistance factor ( $G^* / \sin \delta$ ). Furthermore, a bending beam rheometer (BBR) was used to determine the low-temperature performance of asphalt binder samples wherein the creep stiffness ( $S$ ) and creep rate ( $M$ ) were recorded to evaluate the low-temperature crack resistance of prepared samples. The investigated temperatures were  $-12$  °C and  $-18$  °C.

### 2.2.3. FTIR Spectra Analysis

The FTIR spectra analysis was conducted to characterize and compare the difference in the functional group of asphalt binder samples. A Nicolet iS10 Fourier transform infrared spectrometer produced by Thermo Scientific Co., Ltd., Waltham, MA USA was used. The spectral resolution was  $0.4 \text{ cm}^{-1}$  and the spectral range was  $4000\text{--}400 \text{ cm}^{-1}$ . Lake asphalt is a solid at room temperature; thus, a small amount of TLA powder and potassium bromide crystal were ground and mixed in an agate mortar, and then the samples were pressed by a YP-2 tablet pressing machine to obtain the samples for the FTIR spectra test.

### 2.2.4. Atomic Force Microscope Test

The atomic force microscope (AFM) observation of asphalt binder samples aims to reveal the difference in the microstructure of samples. A Bruker's cloth Dimension ICON AFM was used with a tap model. The scan area was  $90 \mu\text{m} \times 90 \mu\text{m} \times 10 \mu\text{m}$ , the data sampling rate was 50 MHz, and the imaging temperature was 27 °C. The asphalt binder sample was heated to 150 °C and was dropped on a glass slide to obtain the specimen. The bee-like structures in the AFM images were identified by color deference using a commercial software, and then the features of bee-like structure were extracted and calculated. Three parameters, including the maximum bee-like area, the average area of all bee-like structures, and the area ratio of bee-like structures to image area, can be obtained.

### 2.2.5. Performances Test of Recycled Asphalt Mixture

To investigate the effect of hard asphalt binder on the performance of produced asphalt mixtures, the high-temperature rutting test, low-temperature bending test, and fatigue test were conducted. The rutting test was performed under 60 °C ambient temperature. The size of the specimen was  $30 \text{ cm} \times 30 \text{ cm} \times 5 \text{ cm}$ ; each test required three specimens. The high-temperature rutting resistance is characterized by dynamic stability and can be calculated by Equation (1).

$$DS = \frac{(t_2 - t_1) \times N}{d_2 - d_1} \quad (1)$$

where DS is the dynamic stability, load/mm;  $t_1$  and  $t_2$  are the 45th and 60th min, respectively;  $d_1$  and  $d_2$  are the deformations at the 45th and 60th min, respectively; N is the wheeling speed, 42 load/min.

The three-point bending test was performed to evaluate the low-temperature crack resistance of the mixture, as shown in Figure 4. The specimens were 250 mm × 30 mm × 35 mm cuboids, and the loading rate was 50 mm/min. Bending stiffness modulus, bending strength, and maximum bending strain were obtained by the test. Generally, greater maximum bending strain and higher bending strength lead to a better low-temperature performance of the mixture. Furthermore, the fracture energy can be calculated from the area of the stress-strain curve before the material reaches the maximum stress. According to research experience, the evaluation of low-temperature performance by fracture energy is more reasonable than the traditional index of maximum bending strain [22]. Therefore, the fracture energy was selected as the indicator to describe the low-temperature performance of the mixtures.



Figure 4. Three-point bending test of recycled asphalt mixture.

A UTM-35 test machine was used to conduct the three-point fatigue test of the asphalt mixture, and a stress control model under 15 °C with 10 Hz was used. Three specimens were tested under each stress level. The specimens were 250 mm × 30 mm × 35 mm cuboids. The fatigue characteristic is given by Equation (2), and after taking logarithms on both sides of the equation, it can be written as a linear equation, Equation (3). In Equation (3), the intercept  $k$  denotes the average fatigue life of the specimens, and the absolute value of slope  $\sigma$  stands for the decay rate of the fatigue life with an increasing stress ratio.

$$N_f = K \left( \frac{1}{\sigma} \right)^n \tag{2}$$

$$\lg N_f = -n \lg \sigma + k \tag{3}$$

where  $N_f$  is the loading time when specimens break;  $\sigma$  is the stress of repeat loading; 20%, 30%, and 40% of maximum bending stress were used, respectively.

Maximum bending stress of specimens of different mixtures was first tested, and the results are shown in Table 8. A maximum bending stress of 20%, 30%, and 40% was calculated for each type of mixture. We performed the three-point fatigue test of different asphalt mixtures according to the calculation results in Table 8.

Table 8. Bending stress of specimens of different mixtures.

Mixture Type	Maximum Bending Stress (KN)	Stress Ratio		
		0.2	0.3	0.4
AC-20	8.2	1.6	2.5	3.3
EME-20@50%RAP	10.1	2.0	3.0	4.1
EME-20@100%RAP	9.7	1.9	2.9	3.9

### 3. Results and Discussion

#### 3.1. Performance of Hard Asphalt Modified Aged Asphalt

##### 3.1.1. Determining the Optimal Content of Lake Asphalt in Hard Asphalt

The asphalt mixture with a higher modulus tends to have better rutting resistance to traffic. Generally, its modulus can be improved by using hard asphalt binder and additives. This study investigated the feasibility of using TLA as the modifier to increase the modulus of the recycled asphalt mixture. To this end, the dynamic modulus of the EME-20 mixture containing 50% RAP (EME-20@50%RAP) was determined. Its newly-added asphalt binder was hard asphalt made with 30% to 70% proportion of TLA, and the results are shown in Figure 5.

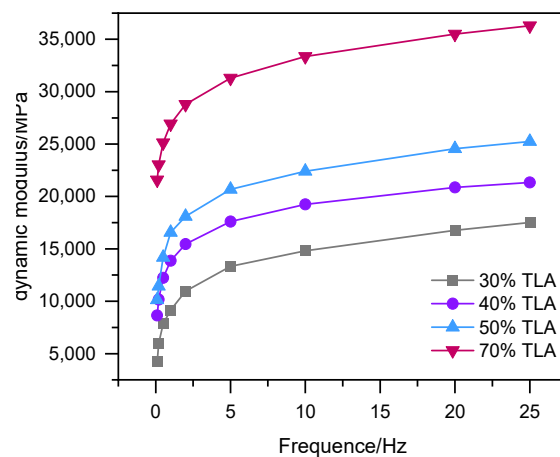


**Figure 5.** Test results of the EME-20 asphalt mixture containing 50% of RAP under 0–25 Hz.

According to Figure 5, the first finding is that the increasing TLA content in hard asphalt binder can significantly increase the modulus of the recycled mixture at every frequency. The optimal TLA content can be obtained when the modulus of RHMA reaches 14,000 MPa under 15 °C, 10 Hz. Therefore, the TLA content in hard asphalt binder was determined as 40%.

##### 3.1.2. FTIR Spectra Analysis of Recycled Asphalt Binder

Figure 6a presents the FTIR spectra of virgin asphalt (VA) and aged virgin asphalt. In Figure 6, a frequency band present at 3800–3500  $\text{cm}^{-1}$  is caused by the vibration of bound water or free water and  $\text{CO}_2$  in ambient air; the strong peaks around 2922–2852  $\text{cm}^{-1}$  are associated with the stretching vibrations in the aliphatic chain of the asphalt binder [23]; the peak at 1600  $\text{cm}^{-1}$  denotes to the vibration of C=C in the benzene skeleton; the peak at 1462 and 1376  $\text{cm}^{-1}$  relates to the deformation vibrations of the aliphatic chain; the peak at 1031  $\text{cm}^{-1}$  is the stretching vibrations of the sulfoxide group (S=O); the peaks at 863, 811, and 747  $\text{cm}^{-1}$  are resulting from the bending vibration of C-H in the aromatic ring. The aging level of asphalt binder samples can be determined by comparing the absorbance of the functional group. The significant difference between three samples is that the transmittance of the functional group of C=C, C=O, and S=O increased after the virgin asphalt binders were aged, and a greater aging level leads to a higher absorbance of those functional groups. The increase in C=O indicates that the oxygen-containing functional groups such as aldehydes, ketones, esters, and carboxylic acids are formed during the aging process of the asphalt binder. Furthermore, the increase in S=O demonstrates that the sulfur element reacts with oxygen to form a polar functional sulfoxide group.

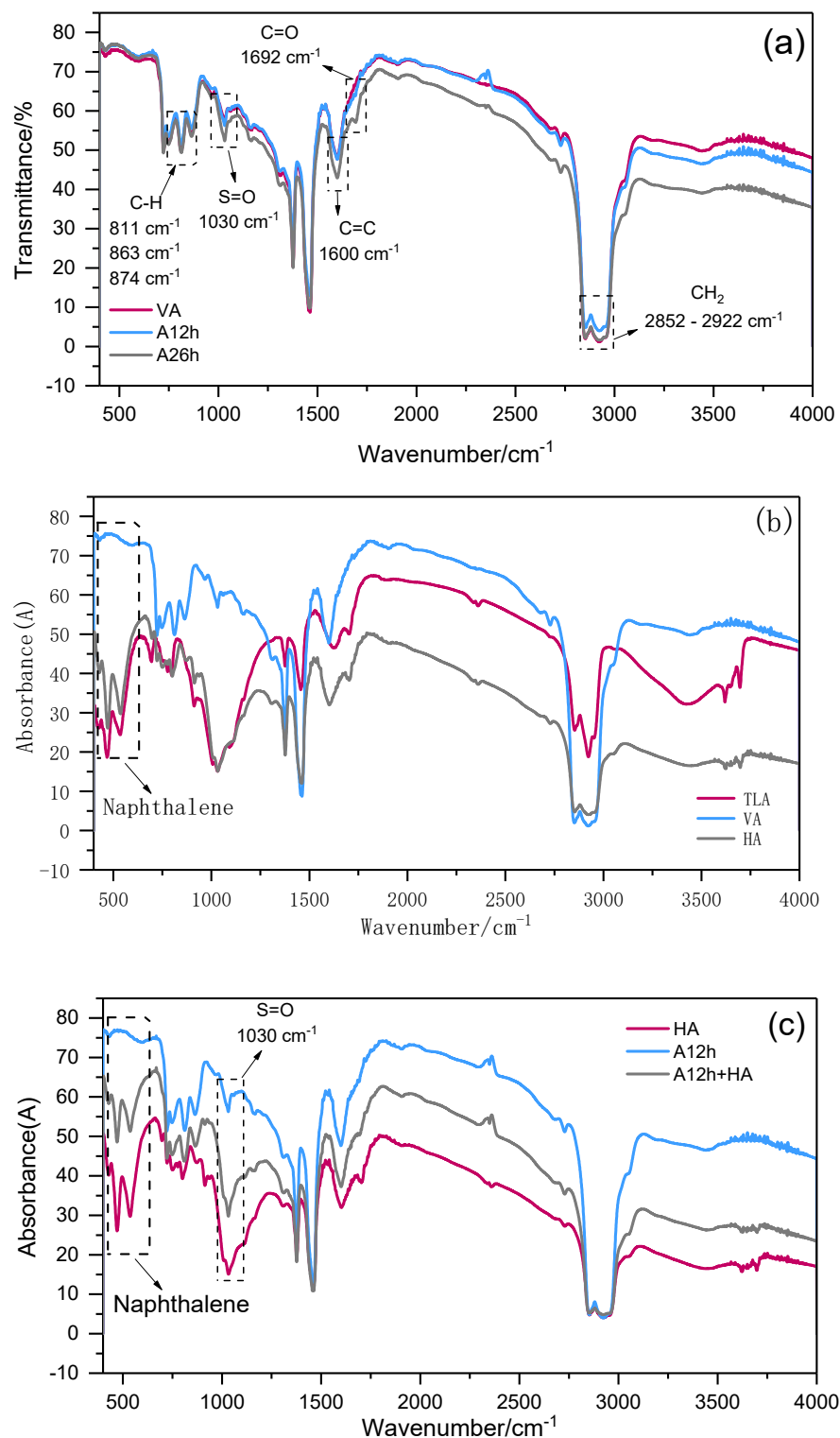
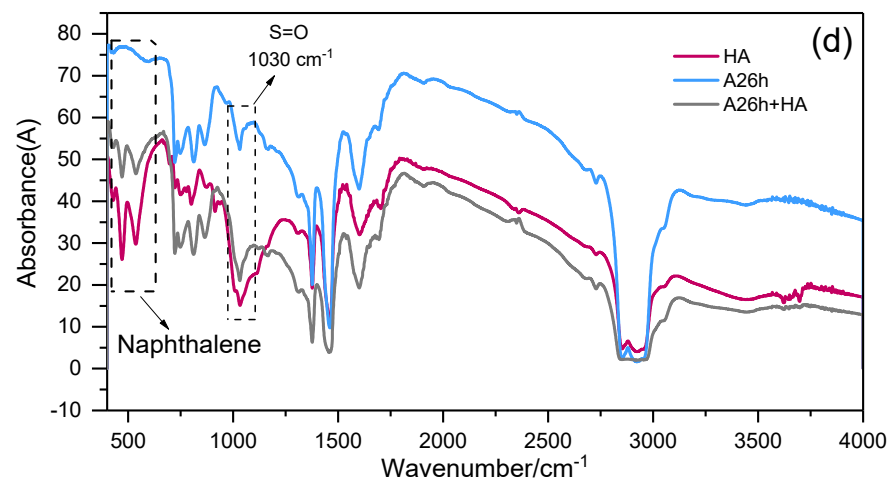


Figure 6. Cont.



**Figure 6.** Fourier transform infrared (FTIR) spectra of virgin and aged asphalt binder samples: (a) VA, A12h, and A26h; (b) TLA, VA, and HA; (c) HA, A12h, and A12h + HA; (d) HA, A26h, and A26h + HA.

Figure 6b illustrates the FTIR spectra of virgin asphalt (VA), Trinidad lake asphalt (TLA), and hard asphalt produced with 60% of VA and 40% of TLA. By comparing the FTIR spectra of VA and TLA, most of the transmittance peaks of TLA are near the absorption peaks of the matrix asphalt. The only new absorption peaks appear at 535, 467, and 428  $\text{cm}^{-1}$ , which correspond to naphthalene functional groups. The addition of a naphthalene functional group is helpful for enhancing the structural strength of petroleum asphalt molecules, which will increase the viscosity of asphalt and enhance the cohesion of asphalt binder and the adhesion with aggregate. In addition, the transmittance peak area of sulfoxide group S=O at 1031  $\text{cm}^{-1}$  of TLA is significantly larger than that of ordinary asphalt binder. The TLA was intensively exposed in an open-air environment, which accelerated the oxidation of TLA. The sulfur and oxygen have sufficient chemical reaction to form more sulfoxide groups. Furthermore, HA and TLA have the same characteristic peaks, in which the transmittance of each functional group in HA is smaller than that of TLA. The above results show that the addition of TLA only changes the proportion of each component in VA, and there is no chemical reaction in this process.

One of the objectives of this work is to rejuvenate the aged asphalt binder using HA containing TLA for producing a high-modulus recycled mixture with high RAP content. Thus, blended asphalt binder samples containing 50% aged asphalt (A12h, A26h) and 50% HA were prepared. Their FTIR spectra are shown in Figure 6c,d. From the effect of HA on aged asphalt, it can be concluded that the sulfoxide group S=O peaks at 1031  $\text{cm}^{-1}$  in both A12h + HA and A26h + HA are sharper compared to that in aged asphalt. This is because the sulfoxide group tends to disintegrate under high temperatures. Furthermore, the appearance of peaks at 535, 467, and 428  $\text{cm}^{-1}$  in both A12h+HA and A26h+HA indicates that the naphthalene functional group in TLA was introduced in the rejuvenated asphalt binder.

### 3.1.3. Analysis of Microstructure Characteristics of Recycled Asphalt Binder

Based on the colloid structure theory of the asphalt binder, asphaltene is considered as the colloid center with a high molecular weight, and the micelles are formed by absorbing the colloidal particles that have greater polarity. The micelles are dispersed in oil [24]. To date, asphaltene is widely believed to be the main component of the convex part of the bee-like structure [25]. By comparing the characteristics of the bee-like structure, the differences in colloid structure of the asphalt binder can be determined. In this section, Figure 7a–c shows virgin asphalt and the aged virgin asphalt after 12 h and 26 h of thermal aging, respectively. The surfaces of aged asphalt samples are rougher than the virgin asphalt when aging time is increased, as shown in Figure 8a. Furthermore, the characteristics

including maximum area, average area, and total area ratio of bee-like structures in A12h and A26h are significantly higher than those in VA. This means thermal aging contributes to a higher content of asphaltene and changes the microstructure of asphalt binder.

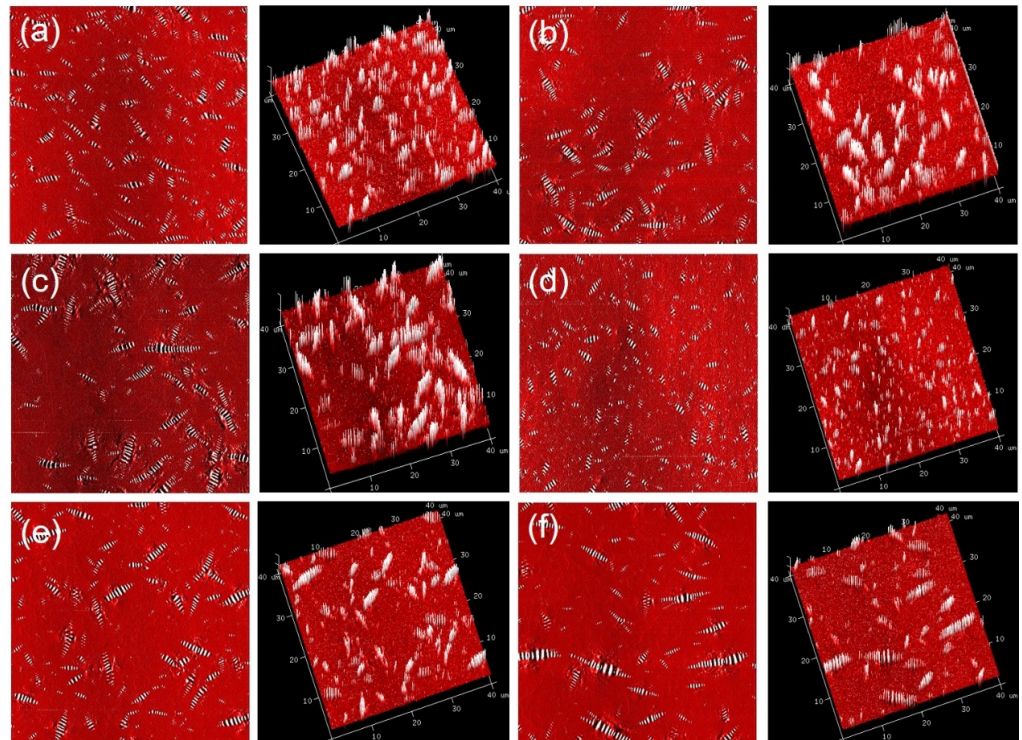


**Figure 7.** Microstructure and 3D structural side view of the asphalt binder imaged using atomic force microscopy (AFM): (a) virgin asphalt, VA; virgin asphalt after (b) 12 h and (c) 26 h thermal aging, denoted by A12h and A26h, respectively; (d) hard asphalt mixed with (e) 12 h and (f) 26 h aged virgin asphalt, denoted by A12h + HA and A26h + HA, respectively.

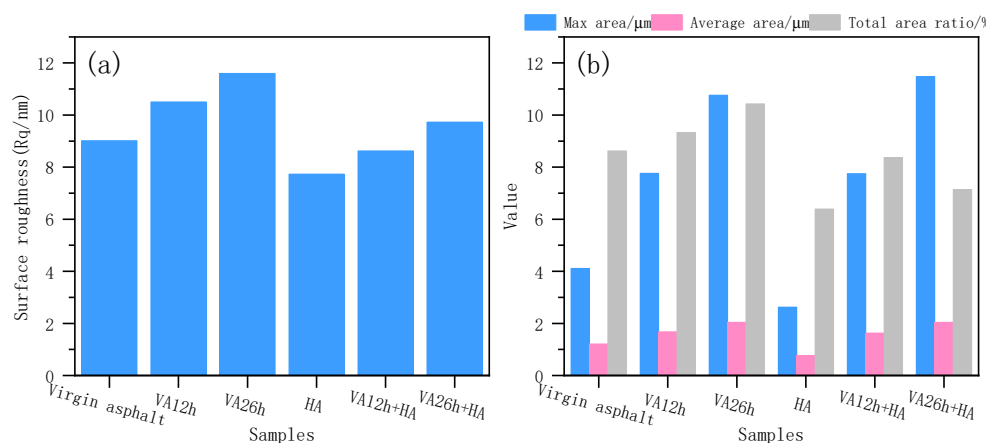


**Figure 8.** Results of the microstructure characteristics of asphalt binder samples: (a) roughness of AFM surface; (b) statistics of bee-like structure.

Furthermore, there is no obvious difference in surface morphology between VA and HA, and they have a similar bee-like structure, as shown in Figure 7a,d. This means the incorporation of TLA in VA did not significantly change the microstructure of VA. To evaluate the rejuvenation effect of HA on aged asphalt with different aging levels, AFM images of HA, A12h + HA, and A26h + HA were obtained, as shown in Figure 7d–f, respectively. By comparing A12h and A12h + HA, as shown in Figure 8b, the characteristic values of the bee-like structure of A12h + HA were determined as slightly lower than

those of A12h, indicating that there was a limited rejuvenation effect on aged asphalt in view of the microstructure. On the other hand, there was a greater improvement in the microstructure of the A26h sample because the characteristic values in A12h + HA were higher than those in A26h. Finally, when HA was added into the asphalt binder with a higher aging degree, the characteristics of the bee-like structure changed dramatically, showing a significant improvement in the maximum area, average area, and total area ratio of bee-like structures.

#### 3.1.4. Rheological Properties of Recycled Asphalt Binder

The creep stiffness ( $S$ ) and creep rate ( $m$ ) of asphalt binder samples were measured using the BBR test at  $-12\text{ }^{\circ}\text{C}$ . Generally, the larger the  $S$  and the lower the  $m$  are, the worse the resistance of the asphalt binder to brittle fracturing in low-temperature environments, which is not conducive to the durability of asphalt pavement. It can be seen from Figure 9a,b that the low-temperature crack resistance of HA was worse than that of VA, which was caused by the addition of TLA. In addition, the low-temperature crack resistance of the virgin asphalt significantly deteriorated after aging, and the  $S$  value of a 26 h was 3.2 times that of the VA. In addition, when 50% HA was added to the aged asphalt, the low-temperature stability of the recycled asphalt binder was significantly worse than that of the VA after the corresponding aging time. Therefore, the use of HA as a rejuvenator for aged asphalt leads to worse low-temperature stability, and this conclusion suggests that the HA modifier is not recommended for use in cold regions.

Figure 9c shows that the high-temperature rutting factor of HA was significantly higher than that of VA, especially at  $58\text{ }^{\circ}\text{C}$  and  $64\text{ }^{\circ}\text{C}$ . In addition, with the increase of the VA aging degree, the rutting factor of A26h asphalt binder increased significantly. The rutting resistance factor of A26h asphalt binder was about seven times higher than that of VA. Furthermore, the rutting factor of asphalt binder with different aging degrees was greatly improved after mixing with 50% HA. For example, at  $58\text{ }^{\circ}\text{C}$ , the rutting factor of A26h + HA was about 20% higher than that of A26. The results of Figure 9a show that HA had a significant effect on improving the rutting resistance of aged asphalt binder. Compared to the conventional asphalt binder, TLA has a high asphaltene and ash content, which contribute to a high stiffness of hard asphalt binder produced with TLA, increasing the high-temperature performance of the hard asphalt binder.

The fatigue factor  $G^*\sin\delta$  was used to compare and evaluate the anti-fatigue characteristics of asphalt binder samples;  $G^*\sin\delta$  refers to the energy lost by the asphalt binder under repeated loads. The smaller the  $G^*\sin\delta$ , the less energy is lost and the better the fatigue resistance. The fatigue factor test results are shown in Figure 9. Figure 9 shows that the fatigue factors of HA and VA were very close, indicating that they have similar fatigue resistance. In addition, with the increase of aging time, the anti-fatigue performance of virgin asphalt decreased significantly. For example, the fatigue factor of A26h was about 30 times higher than that of VA. The reason is that as the aging time increased, the asphaltene and gum content in the asphalt binder increased, and the saturated and aromatic components decrease, resulting in an increase in the complex modulus and the fatigue factor. In addition, when HA was mixed with aged asphalt, its fatigue factor was slightly higher than that of aged asphalt. For instance, the fatigue factor of A26h + HA was about 10% higher than that of A26h. The above results show that the fatigue performance of aged asphalt decreases with the addition of HA. This is due to the fact that TLA has a relatively large ash content. After the ash particles precipitate, the elasticity and toughness of HA are reduced, which leads to a decrease in fatigue performance. From this point of view, rejuvenating the aging asphalt binder using HA is not preferred for high-traffic pavements.

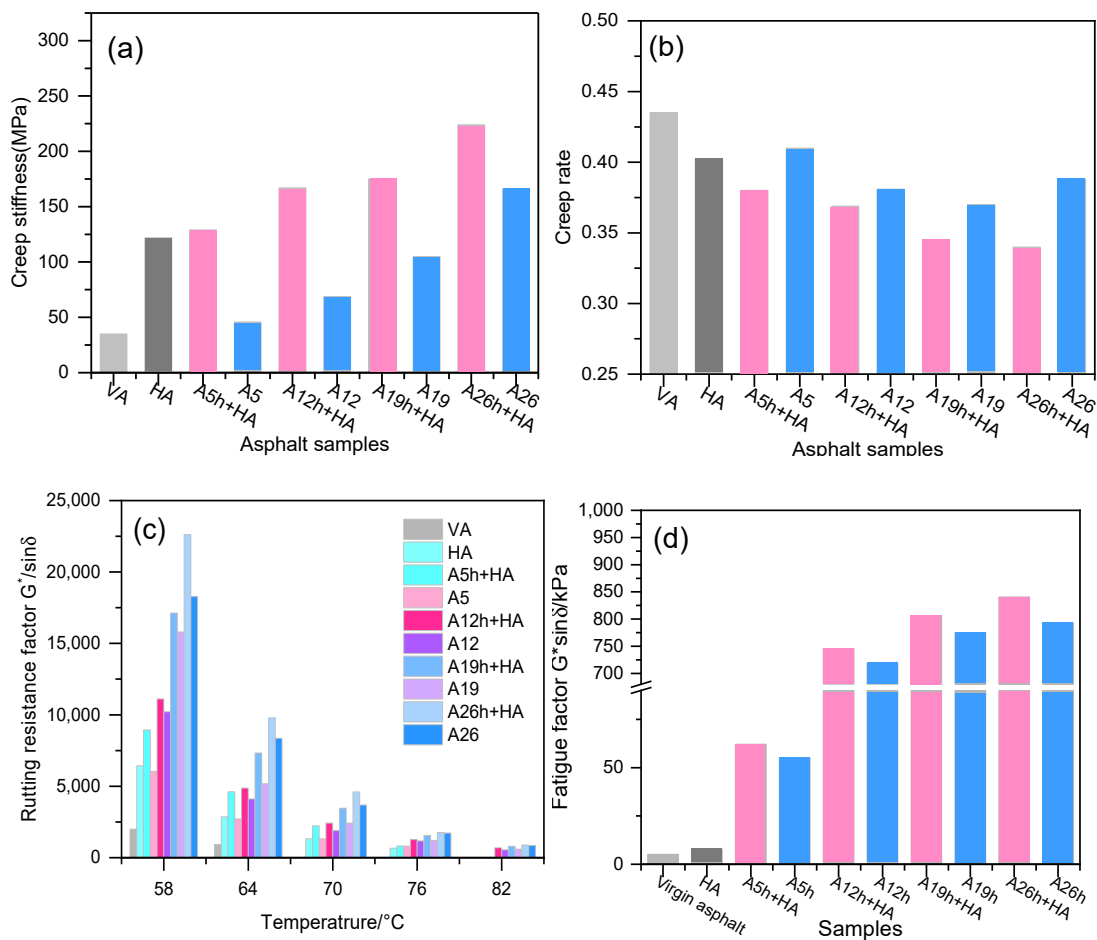


Figure 9. Rheological properties of recycled asphalt binder: (a) creep stiffness; (b) creep rate; (c) rutting factor; (d) fatigue factor.

### 3.2. Performance of Hot-Mix Recycled Asphalt Mixture Containing Hard Asphalt

Three kinds of asphalt mixtures were prepared to reveal the difference in performance between the conventional and the hot-mix recycled asphalt mixture (RHMA). The RHMA was designed based on the principle of the high-modulus mixture using the hard asphalt as a binder, containing 50% and 100% RAP, denoted by EME-20@50% and EME-20@100%, respectively. Figure 10a indicates that EME-20@100% and EME-20@50% had similar dynamic stability (DS). Compared with the ordinary asphalt mixture containing hard asphalt binder, the high-temperature performance was lower.

As shown in Figure 10b, the AC-20 specimens had the highest bending strain compared to others, indicating the conventional AC-20 could bear a higher deformation than EME-20 specimens. Furthermore, there was no significant difference between EME-20@50% and EME-20@100%, which means that they have a similar deformation resistance. Figure 10c shows the bending strength of tested samples; the results indicate that AC-20 has the lowest bending strength. In summary, the specimens designed using the concept of high-modulus asphalt mixture were stiffer than the conventional one, which it led to a greater bending strength and lower bending strain. To compare the low-temperature performance of samples, fracture energy was used, which can reveal the performance differences in terms of energy; the results are shown in Figure 10d. Figure 10d shows that EME-20@50% had a similar fracture energy to AC-20, indicating that the incorporation of hard asphalt and 50% RAP had no negative effect on the low-temperature cracking resistance of the asphalt mixture. Moreover, when the RAP content was increased to 100%, the fracture energy of EME-20@100% increased by 23% compared to that of AC-20 due to the fine gradation and high asphalt binder content.

Moreover, Figure 10e suggests that EME-20@100% had the highest fatigue life under different stress ratios. The fatigue lives of EME-20@100% and EME-20@50% were both higher than that of AC-20, but the slope of the fatigue curve was greater, indicating that they were more sensitive to stress. This paper used a stress-controlled mode to carry out the fatigue experiment. The experimental results obtained under strain-controlled mode may be different, which should be further studied. In summary, fine gradation and a high asphalt binder content improved low-temperature crack resistance and fatigue life while maintaining a good high-temperature performance of RHMA. Therefore, the high modulus design concept can be adopted to increase RAP content in recycling.

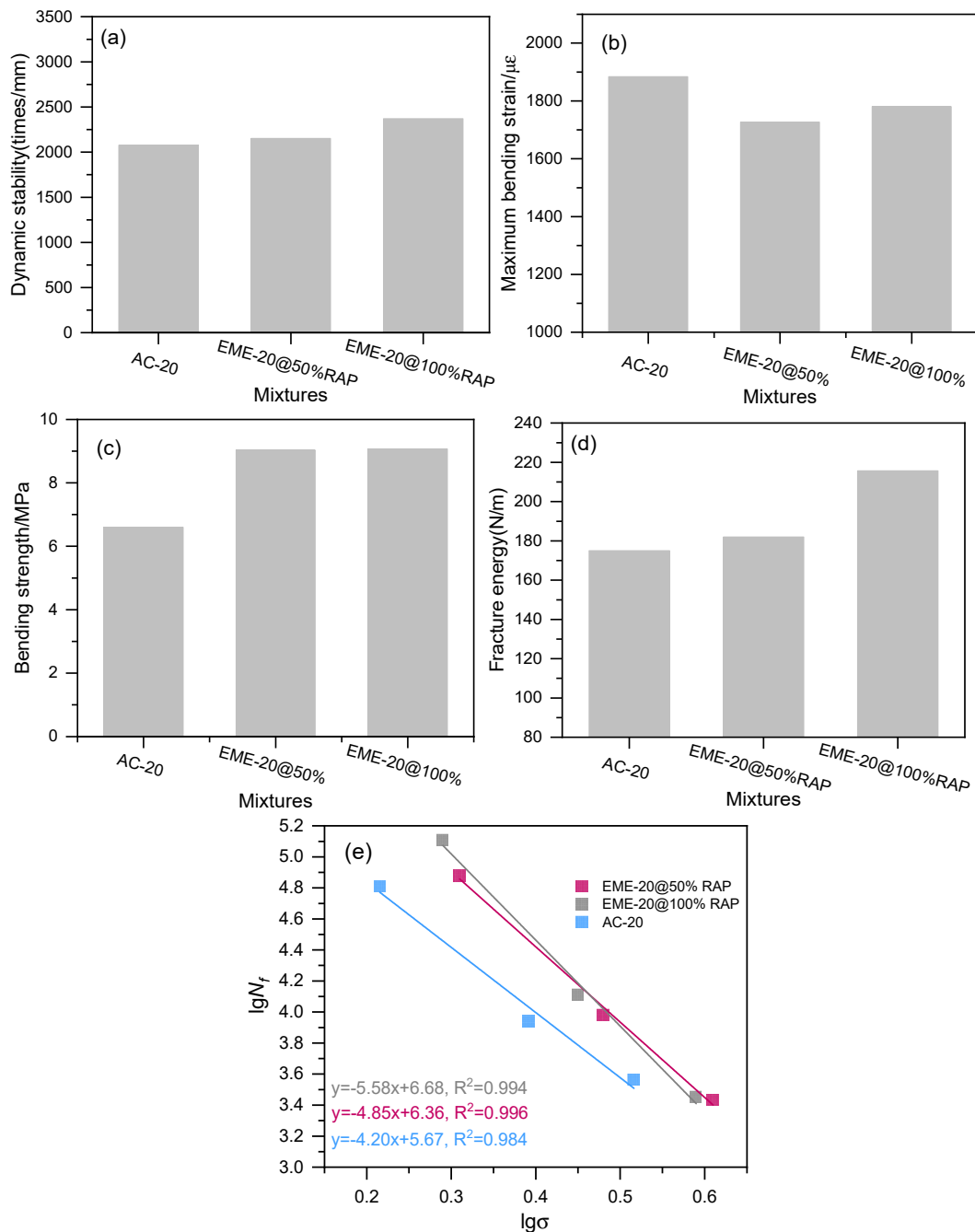


Figure 10. Performance of hot-mix recycled asphalt mixture containing hard asphalt: (a) High-temperature rutting resistance; (b) Maximum bending strain; (c) Bending strength; (d) Fracture energy; (e) Fatigue performance.

#### 4. Conclusions

In this paper, the modification mechanism, microstructure, and rheological properties of hard asphalt binder produced by mixing TLA and VA were analyzed using infrared spectroscopy, atomic force microscopy, and DSR and BBR experiments. The performance of RHMA produced with hard asphalt was tested, and the following conclusions can be drawn.

- (1) The addition of TLA leads to a change in the component proportion of asphalt binder, but no new functional groups are produced; the addition of TLA leads to a decrease in the number and total area of bee structures, which indicates that lake asphalt changes the interaction between asphaltene and other asphalt molecules. This is conducive to the dissolution of asphaltene and forms a more stable system.
- (2) The low-temperature performance of recycled asphalt binder and aged asphalt binder has the same change rule. With the extension of aging time, the low-temperature performance of recycled asphalt binder gradually decreases, the high-temperature performance increases, and fatigue damage develops rapidly.
- (3) As high-modulus asphalt mixture and RAP have similarity in terms of asphalt binder performance and fine gradation, adopting the high modulus design concept for recycling can increase the RAP content. Through the optimization of gradation and the use of hard asphalt, the high- and low-temperature performance and anti-fatigue performance of 100% recycled asphalt mixture are better than when using the AC-20 mixture. Thus, recycling with a high-modulus asphalt mixture design concept to increase the RAP content is feasible.

**Author Contributions:** Conceptualization, J.Z. and Y.Z.; methodology, J.Z., J.L. and G.L.; formal analysis, J.Z., J.L., G.L. and T.Y.; data curation, J.Z. and J.L.; writing—original draft preparation, J.Z., G.L., and T.Y.; writing—review and editing, G.L., T.Y. and Y.Z. All authors have read and agreed to the published version of the manuscript.

**Funding:** This research was funded by the National Natural Science Foundation of China through project 51378123 and the Graduate Research and Innovation Projects of Jiangsu Province (KYLX\_0167).

**Institutional Review Board Statement:** Not applicable.

**Informed Consent Statement:** Not applicable.

**Data Availability Statement:** No new data were created or analyzed in this study. Data sharing is not applicable to this article.

**Acknowledgments:** The authors would like to acknowledge the financial support provided by the National Natural Science Foundation of China through project 51378123. The present article is also supported by the Fundamental Research Funds for the Graduate Research and Innovation Projects of Jiangsu Province (KYLX\_0167). The funding supported the FTIR spectra analysis and atomic force microscope test. The authors thank them for their support in the development of the project.

**Conflicts of Interest:** The authors declare no conflict of interest.

#### References

1. Debbarma, S.; Ransinchung, G.D. Achieving sustainability in roller compacted concrete pavement mixes using reclaimed asphalt pavement aggregates—State of the art review. *J. Clean. Prod.* **2021**, *287*, 125078. [[CrossRef](#)]
2. Georgiou, P.; Loizos, A. Environmental assessment of warm mix asphalt incorporating steel slag and high reclaimed asphalt for wearing courses: A case study. *Road Mater. Pavement Des.* **2021**, *22*, S662–S671. [[CrossRef](#)]
3. Wang, H.; Thakkar, C.; Chen, X.; Murrel, S. Life-cycle assessment of airport pavement design alternatives for energy and environmental impacts. *J. Clean. Prod.* **2016**, *133*, 163–171. [[CrossRef](#)]
4. Wang, F.; Xie, J.; Wu, S.; Li, J.; Barbieri, D.M.; Zhang, L. Life cycle energy consumption by roads and associated interpretative analysis of sustainable policies. *Renew. Sustain. Energy Rev.* **2021**, *141*, 110823. [[CrossRef](#)]
5. Pradyumna, T.A.; Mittal, A.; Jain, P.K. Characterization of Reclaimed Asphalt Pavement (RAP) for Use in Bituminous Road Construction. *Procedia Soc. Behav. Sci.* **2013**, *104*, 1149–1157. [[CrossRef](#)]
6. Hussain, A.; Yanjun, Q. Effect of Reclaimed Asphalt Pavement on the Properties of Asphalt Binders. *Procedia Eng.* **2013**, *54*, 840–850. [[CrossRef](#)]

7. Gao, J.; Yang, J.; Yu, D.; Jiang, Y.; Ruan, K.; Tao, W.; Sun, C.; Luo, L. Reducing the variability of multi-source reclaimed asphalt pavement materials: A practice in China. *Constr. Build. Mater.* **2021**, *278*, 122389. [[CrossRef](#)]
8. Delorme, J.L.; De la Roche, C.; Wendling, L. *LPC Bituminous Mixtures Design Guide*; Laboratoire Central des Ponts et Chaussées: Paris, France, 2007.
9. Yan, J.; Zhang, Z.; Zhu, H.; Li, F.; Liu, Q. Experimental Study of Hot Recycled Asphalt Mixtures with High Percentages of Reclaimed Asphalt Pavement and Different Recycling Agents. *J. Test. Eval.* **2014**, *42*, 1183–1190. [[CrossRef](#)]
10. Gao, L.; Li, H.; Xie, J.; Yu, Z.; Charmot, S. Evaluation of pavement performance for reclaimed asphalt materials in different layers. *Constr. Build. Mater.* **2018**, *159*, 561–566. [[CrossRef](#)]
11. Hu, X.; Nie, Y.; Feng, Y.; Zheng, Q. Pavement Performance of Asphalt Surface Course Containing Reclaimed Asphalt Pavement (RAP). *J. Test. Eval.* **2012**, *40*, 1162–1168. [[CrossRef](#)]
12. Wang, H.; Dang, Z.; Li, L.; You, Z. Analysis on fatigue crack growth laws for crumb rubber modified (CRM) asphalt mixture. *Constr. Build. Mater.* **2013**, *47*, 1342–1349. [[CrossRef](#)]
13. Al-Saffar, Z.H.; Yaacob, H.; Satar, M.K.I.M.; Saleem, M.K.; Lai, J.C.; Putra Jaya, R. A review on rejuvenating materials used with reclaimed hot mix asphalt. *Can. J. Civ. Eng.* **2021**, *48*, 233–249. [[CrossRef](#)]
14. Yu, X.; Zaumanis, M.; dos Santos, S.; Poulikakos, L.D. Rheological, microscopic, and chemical characterization of the rejuvenating effect on asphalt binders. *Fuel* **2014**, *135*, 162–171. [[CrossRef](#)]
15. Yousefi, A.; Behnood, A.; Nowruzzi, A.; Haghshenas, H. Performance evaluation of asphalt mixtures containing warm mix asphalt (WMA) additives and reclaimed asphalt pavement (RAP). *Constr. Build. Mater.* **2021**, *268*, 121200. [[CrossRef](#)]
16. Wróbel, M.; Wozzuk, A.; Ratajczak, M.; Franus, W. Properties of reclaimed asphalt pavement mixture with organic rejuvenator. *Constr. Build. Mater.* **2021**, *271*, 121514. [[CrossRef](#)]
17. Yan, J.; Leng, Z.; Ling, C.; Zhu, J.; Zhou, L. Characterization and comparison of high-modulus asphalt mixtures produced with different methods. *Constr. Build. Mater.* **2020**, *237*, 117594. [[CrossRef](#)]
18. Zhu, J.; Ma, T.; Fan, J.; Fang, Z.; Chen, T.; Zhou, Y. Experimental study of high modulus asphalt mixture containing reclaimed asphalt pavement. *J. Clean. Prod.* **2020**, *263*, 121447. [[CrossRef](#)]
19. Ma, T.; Wang, H.; Huang, X.; Wang, Z.; Xiao, F. Laboratory performance characteristics of high modulus asphalt mixture with high-content RAP. *Constr. Build. Mater.* **2015**, *101*, 975–982. [[CrossRef](#)]
20. Liu, J.; Yan, K.; Liu, J.; Guo, D. Evaluation of the characteristics of Trinidad Lake Asphalt and Styrene–Butadiene–Rubber compound modified binder. *Constr. Build. Mater.* **2019**, *202*, 614–621. [[CrossRef](#)]
21. Fang, M.; Park, D.; Singuranayo, J.L.; Chen, H.; Li, Y. Aggregate gradation theory, design and its impact on asphalt pavement performance: A review. *Int. J. Pavement Eng.* **2018**, *20*, 1408–1424. [[CrossRef](#)]
22. Mull, M.A.; Stuart, K.; Yehia, A. Fracture resistance characterization of chemically modified crumb rubber asphalt pavement. *J. Mater. Sci.* **2002**, *37*, 557–566. [[CrossRef](#)]
23. Wang, J.; Yuan, J.; Kim, K.W.; Xiao, F. Chemical, thermal and rheological characteristics of composite polymerized asphalts. *Fuel* **2018**, *227*, 289–299. [[CrossRef](#)]
24. Zhang, H.; Wang, Y.; Yu, T.; Liu, Z. Microstructural characteristics of differently aged asphalt samples based on atomic force microscopy (AFM). *Constr. Build. Mater.* **2020**, *255*, 119388. [[CrossRef](#)]
25. Wang, Y.; Zhang, H. Influence of asphalt microstructure to its high and low temperature performance based on atomic force microscope (AFM). *Constr. Build. Mater.* **2021**, *267*, 120998. [[CrossRef](#)]